Mutations in the *SUP-PF-1* Locus of *Chlamydomonas reinhardtii* Identify a Regulatory Domain in the β-Dynein Heavy Chain

Mary E. Porter,* Julie A. Knott,* Lynne C. Gardner,* David R. Mitchell,‡ and Susan K. Dutcher§

*Department of Cell Biology and Neuroanatomy, University of Minnesota Medical School, Minneapolis, Minnesota 55455; ‡Department of Anatomy and Cell Biology, State University of New York Health Science Center, Syracuse, New York 13210; and §Department of Molecular, Cellular, and Developmental Biology, University of Colorado at Boulder, Boulder, Colorado 80309-0347

Abstract. We have characterized a group of regulatory mutations that alter the activity of the outer dynein arms. Three mutations were obtained as suppressors of the paralyzed central pair mutant *pf6* (Luck, D. J. L., and G. Piperno. 1989. Cell Movement. pp. 49–60), whereas two others were obtained as suppressors of the central pair mutant *pf16*. Recombination analysis and complementation tests indicate that all five mutations are alleles at the *SUP-PF-1/ODA4* locus and that each allele can restore motility to radial spoke and central pair defective strains. Restriction fragment length polymorphism analysis with a genomic probe for the β-dynein heavy chain (DHC) gene confirms that this locus is tightly linked to the β-DHC gene. Although all five mutant *sup-pf-1* alleles alter the activity of the outer dynein arm as assayed by measurements of flagellar motility, only two alleles have a discernable polypeptide defect by SDS-PAGE. We have used photolytic and proteolytic cleavage procedures to localize the polypeptide defect to an ~100-kD domain downstream from the last putative nucleotide binding site. This region is encoded by ~5 kb of genomic DNA (Mitchell, D. R., and K. Brown. 1994. *J. Cell Sci.* 107:653–644). PCR amplification of wild-type and mutant DNA across this region identified one PCR product that was consistently smaller in the *sup-pf-1* DNA. Direct DNA sequencing of the PCR products revealed that two of the *sup-pf-1* mutations are distinct, in-frame deletions. These deletions occur within a region that is predicted to encode a small α-helical coiled-coil domain of the β-DHC. This domain may play a role in protein–protein interactions within the outer dynein arm. Since both the size and location of this domain have been conserved in all axonemal and cytoplasmic DHCs sequenced to date, it presumably performs a common function in all dynein isoforms.

THE dynein ATPases are a family of motor enzymes that provide the driving force for ciliary and flagellar motility and contribute to microtubule-based movements inside cells (reviewed in Porter and Johnson, 1989; Vallee, 1993). These enzymes convert the energy derived from nucleotide binding and hydrolysis into the directed movement of cellular cargoes toward the minus ends of microtubules (reviewed in Porter and Johnson, 1989). All dyneins characterized thus far are extremely large (>1–2 MD), multisubunit protein complexes. The large size and subunit complexity have hampered the identification of functional domains within the dyneins. However, the numerous flagellar mutations that affect dynein structure and function in *Chlamydomonas*, coupled with the recently published sequences of dynein heavy chains (DHCs)[1], provide new opportunities for the identification of functional domains within these very large proteins.

In *Chlamydomonas*, the outer dynein arms are composed of three heavy chains (α, β, and γ), two intermediate chains (70 and 78 kD), and several light chains (8–20 kD). Mutations that alter the assembly or activity of the outer arm identify 13 different genes. In most cases, these mutations result in the loss of all outer arm polypeptides from the axoneme, and the mutant gene product can not be easily identified (reviewed in Luck and Piperno, 1989). One locus, *ODA6*, has been identified as the structural gene for the 70-kD intermediate chain by rescue of the mutant phenotype with a wild-type copy of the gene (Mitchell and Kang, 1991). Another locus, *ODA11*, has been linked to the structural gene for the α-DHC by restriction fragment length polymorphism (RFLP) mapping techniques (Sakakibara et al., 1991). A third locus, *ODA4*, is thought to be the structural gene for the β-DHC on the basis of its linkage to an unusual mutation known as *sup-pf-1* (Luck and Piperno, 1989).

The first *sup-pf-1* allele was isolated as an extragenic suppressor of the paralyzed central pair mutant *pf6* (Huang et al., 1982). Mutations that disrupt the radial spokes or central pair structures generally lead to flagellar paralysis by a

Address all correspondence to Mary E. Porter, Department of Cell Biology and Neuroanatomy, University of Minnesota Medical School, 4-135 Jackson Hall, 321 Church St. SE, Minneapolis, MN 55455. Phone: (612) 626-1901; fax: (612) 624-8118.

1. *Abbreviations used in this paper*: cM, centimorgan; DHC, dynein heavy chain; DRC, dynein regulatory complex; HUV, heavy UV vanadate cleavage fragment; LUV, light UV vanadate cleavage fragment; RFLP, restriction fragment length polymorphism.

mechanism that appears to involve a global inactivation of dynein arm activity (Smith and Sale, 1992). Extragenic suppressors short circuit this inhibition and allow for some dynein arm activity in the absence of a normal signal from the radial spoke-central pair complex (Huang et al., 1982). Although many extragenic suppressors affect inner arm structures (Mastronarde et al., 1992; Piperno et al., 1992; Porter et al., 1992), the *sup-pf-1-1* mutation appears to alter the activity of the outer dynein arm (Brokaw et al., 1982). In *sup-pf-1-1* strains, the outer dynein arms still assemble into the flagellar axoneme, but the flagellar beat frequency is reduced to ~50% of wild-type levels (Brokaw et al., 1982). These motility defects are similar but not identical to those observed in *oda4* cells (Brokaw and Kamiya, 1987), but the only discernable polypeptide defect is an altered electrophoretic mobility of the β-DHC in some *sup-pf-1* alleles (reviewed in Luck and Piperno, 1989). Because this variant form of the β-DHC (β′) coassembles with its wild-type counterpart into the axonemes of heterozygous dikaryons, it has been proposed that the *sup-pf-1-1* mutation represents a lesion in the structural gene for the β-DHC, as opposed to a defect in posttranslational modification (Huang et al., 1982). If so, this mutation would identify a domain of the β-DHC that modulates both the flagellar beat frequency and the response of the outer arm to signals from the radial spoke/central pair complex.

The DHCs contain the primary sites of ATP binding and hydrolysis and are also thought to contain the ATP-sensitive microtubule-binding site or motor domain. Sequence analyses have revealed the presence of four highly conserved phosphate-binding sites or P loops, but little has been garnered about the position of other functional domains from the sequences (Gibbons et al., 1991; Ogawa, 1991; Mitchell and Brown, 1994). The characterization of several mutant alleles within a single DHC gene could therefore provide new insights into the locations of such domains within these exceptionally large proteins. In this study, we demonstrate that five mutations that alter the activity of the outer dynein arm are all alleles at the β-DHC locus. For two of these alleles, we have localized the site of the mutant defects to a distinct domain within the polypeptide sequence. These are the first DHC mutations to be characterized at the primary sequence level. The polypeptide domain identified by these mutations appears to play a role in the regulation of force production and flagellar motility by the outer dynein arm.

Materials and Methods

Mutant Strains

All strains used in this study are listed in Table I. The strain *oda4* (*oda38*) (Kamiya, 1988) was obtained from the *Chlamydomonas* Genetics Center (Duke University, Durham, NC). Three *sup-pf-1* alleles (*R6*, *R13*, and *D22*) were generously provided by Dr. David Luck (The Rockefeller University, New York), and two new *sup-pf-1* alleles were identified as described below. *R6* and *R13* were obtained by UV mutagenesis, whereas *D22* was obtained by exposure to the chemical mutagen diepoxybutane (Luck and Piperno, 1989; Luck, D., personal communication). As part of the effort to standardize genetic nomenclature in *Chlamydomonas*, we have designated the multiple alleles at the *SUP-PF-1* locus by a hyphen and a number.

Genetic Analysis

New mutations were mapped to their genetic loci by recombination analysis of tetrad progeny using standard techniques (Levine and Ebersold, 1960; Harris, 1989). Dominance and complementation tests were performed by constructing stable diploid cell lines (Ebersold, 1967). Each mutation was crossed into an arginine-requiring background (either the intraallelic *arg2* or *arg7* allele), and the appropriate diploid was selected on medium lacking arginine (Ebersold, 1967). At least four independently isolated cell lines were examined for each diploid construction, and all diploids were demonstrated to be mating type minus.

Isolation of New sup-pf-1 Alleles

31 extragenic suppressors of the temperature-sensitive *pf16BR3* mutant strain (Dutcher et al., 1984) were obtained by ultraviolet irradiation of gametic cells for 45 (Luck et al., 1977) and then screening 20-ml liquid cultures for swimming cells at the restrictive temperature of 32°C (Porter et al., 1992). 11 of the revertants are bypass suppressors; they rescue the flagellar paralysis associated with the *pf16BR3* mutation without restoring the missing central pair polypeptides. Initial backcrosses of these revertants to a wild-type strain indicated that two of the bypass suppressors (*RR5* and

Table I. Characteristics of Mutant Strains Used in This Study

Strain (isolate)	Motility phenotype	Axonemal defect	Reference
C. smithii (CC1373)	Wild type		Harris (1989)
wild-type (137c)	Wild type		Harris (1989)
pf6	Paralyzed, twitch	C1 central pair projection	Dutcher et al. (1984)
pf16BR3 (ncs66R3)	Paralyzed, twitch	C1 central pair microtubule	Dutcher et al. (1984)
pf28 (oda2)	Slow swimming	Outer arm missing	Mitchell and Rosenbaum (1985)
oda4 (oda38)	Slow swimming	Outer arm missing	Kamiya (1988)
oda11	Slow swimming	α-DHC missing	Sakakibara et al. (1991)
sup-pf-1-1 (R6)	Slow swimming	Altered β-DHC (β′)	Huang et al. (1982)
sup-pf-1-2 (D22)	Slow swimming	Altered β-DHC (β′)	Luck and Piperno (1989)
sup-pf-1-3 (R13)	Slow swimming	None detected	Luck and Piperno (1989)
sup-pf-1-4 (RR5)	Slow swimming	None detected	This study
sup-pf-1-5 (RR48)	Slow swimming	None detected	This study
pf9-2	Abnormal waveform, slow swimming	I1 inner arm subunit	Porter et al. (1992)
pf9-2 sup-pf-1-1	Slow wobble	I1 inner arm subunit, altered β-DHC	Porter et al. (1992)

RR48) are linked to the original *pf16BR3* mutation on linkage group IX (tetrad ratios of 7:0:1 and 14:0:1, respectively). These two suppressors were selected for further study as possible new alleles of the *SUP-PF-1* locus.

Measurements of Flagellar Motility

The phenotypes of motility mutations were scored by phase contrast microscopy on a standard or Axioscop (Carl Zeiss, Inc., Thornwood, NY) microscope using a 40× objective and a 10× eyepiece for a final magnification of 400. Measurements of swimming velocities were made from video recordings (BC-1000 VCR; Mitsubishi Corp., Tokyo) of live cells using a C2400 Newvicon camera and Argus 10 video processor (Hamamatsu Photonic Systems Corp., Bridgewater, NJ) calibrated with a stage micrometer. Analysis of flagellar beat frequencies was performed by dark-field microscopy using a stroboscopic light source as described by Mitchell and Kang (1991).

RFLP Analysis

C. reinhardtii and *C. smithii* are two interfertile *Chlamydomonas* strains known to be polymorphic at the DNA sequence level (Ranum et al., 1988). Molecular markers can be mapped relative to genetic markers by examining their cosegregation in crosses between these two strains. Genomic DNA was isolated from these two strains, digested with a series of restriction enzymes, and probed with a 2.8-kb fragment of the β-DHC gene known as *Dhl* (Williams et al., 1986; Mitchell, 1989; Mitchell and Brown, 1994). Scorable RFLPs were identified with the enzymes Msp I and Hinf I.

63 tetrads were dissected from a cross between a *C. reinhardtii* strain carrying the *sup-pf-1-1* (*R6*) and *sr1* (streptomycin resistance) mutations and a wild-type strain of *C. smithii*. All of the tetrad products were scored with respect to their flagellar phenotypes by phase contrast light microscopy. Streptomycin resistance was determined by growth in presence of 25 μg/ml streptomycin sulfate.

DNA was isolated from all four progeny of 18 tetrads and from a single randomly chosen individual of an additional 45 tetrads using the procedures described in Johnson and Dutcher (1991). The DNA samples were digested with HinfI, separated on 0.8% agarose gels, transferred to Zetabind, and probed with a ^{32}P-labeled *Dhl* fragment using standard techniques (Sambrook et al., 1989).

Cell Culture, Axoneme Isolation, and Dynein Purification

Methods used for the culture of cells, the isolation of axonemes, and the purification of dyneins by sucrose density gradient centrifugation have been previously described in detail (Porter et al., 1992). These procedures were essentially after Luck et al. (1977); Witman (1986); King et al. (1986). Some samples of outer arm αβ subunits were prepared from mutant strains that lack the cosedimenting I1 inner arm subunits (e.g., *pf9-2* and *pf9-2 sup-pf-1-1*) (Porter et al., 1992).

Biochemical Procedures

ATPase activity was measured in the presence of 0.3 M KCl, 30 mM Tris-HCl, pH 8.0, 5 mM $MgSO_4$, 0.1 mM EGTA, and 1 mM ATP. Inorganic phosphate released was determined colorimetrically by the method of Waxman and Goldberg (1982). Protein concentrations were determined by the method of Bradford (1976) using BSA as a standard.

Photolytic and Proteolytic Cleavage of DHCs

V1 Cleavage. Sucrose density gradient-purified αβ outer arm subunits in HMEEK buffer (30 mM Hepes, pH 7.4, 5 mM $MgSO_4$, 1 mM EGTA, 0.1 mM EDTA, 25 mM KCl, 1 mM DTT, and 2.5 μg/ml aprotinin, leupeptin, and pepstatin) were UV-irradiated in the presence and absence of 1 mM MgATP and 100 μM sodium vanadate for 1 h at 4°C. 50–100-μl aliquots were placed on Parafilm over an ice bath and irradiated with a long wavelength UV light source (model EN-28 lamp; Spectronics Corp., Westbury, NY) at a distance of 3 cm. The resulting products are designated the heavy UV vanadate cleavage fragment (HUV) and the light UV vanadate cleavage fragment (LUV) based on their relative sizes.

V2 Cleavage. Gradient-purified αβ subunits were dialyzed overnight against 2× 1 liter changes of 10 mM Hepes, 0.1 mM EDTA to remove Mg^{2+}. $MnSO_4$ and sodium vanadate were added to a final concentration of 1 mM and 500 μM respectively, and the samples were then UV-irradiated for 1 h at 4°C.

Chymotryptic Cleavage. Gradient-purified αβ subunits were dialyzed overnight against 10 mM Tris-HCl, pH 7.5, 25 mM NaCl, 0.1 mM EDTA. 60-μl samples containing 1.5 μg of protein were incubated with 5–100 ng of α-chymotrypsin (C-3142; Sigma Chemical Co., St. Louis, MO) for 5 min at room temperature. Digests were stopped by the addition of 15 μl of 5× SDS electrophoresis sample buffer and boiling for 2 min. Samples were then loaded immediately on SDS-polyacrylamide gels.

SDS-PAGE

Purified axonemes prepared from haploid and diploid strains were analyzed on 3–5% polyacrylamide, 2–8 M urea gradient gels (Laemmli, 1970; King et al., 1986). Sucrose gradient–purified dynein fractions were analyzed on the same gel system and also on 0–2.4 M glycerol, 5–10, or 5–15% polyacrylamide gradient gels containing standard or reduced amounts of bisacrylamide. Some samples were also analyzed on 3.2–5% polyacrylamide, 2–8 M urea gradient gels using the Neville-based buffer system as described by Piperno and Luck (1979).

PCR Amplification of DNA and Direct DNA Sequencing

200 ng of genomic DNA samples prepared from wild-type and mutant strains were used as templates in 100-μl PCR reactions containing 1 μM primers, 0.2 mM NTPs, 1× reaction buffer (20 mM Tris-HCl, pH 8.2, 10 mM KCl, 6 mM $(NH_4)_2SO_4$, 1.5 mM $MgCl_2$, and 0.1% Triton-X-100), and 2.5 U *Pfu* DNA polymerase (Stratagene, La Jolla, CA). *Pfu* DNA polymerase was chosen because of its increased fidelity of DNA synthesis (>12-fold over *Taq* DNA polymerase according to the manufacturer's specifications). The following primer pairs were used: B1 (nt 13300-13319) and B2 (antisense nt 14052-14071); B3 (nt 14054-14073) and B4 (antisense nt 14637-14656); B5 (nt 14603-14622) and B6 (antisense 15266-15285); B7 (nt 15266-15285) and B8 (antisense nt 16159-16178); B9 (nt 16125-16144) and B10 (antisense nt 16799-16818); B11 (nt 16694-16713) and B12 (antisense nt 17698-17717) (see Mitchell and Brown [1994] for nucleotide positions). After an initial 5-min denaturation step at 95°C, the reactions underwent 30 cycles of amplification at 58°C or 62°C for 2 min, 74°C for 3 min, and 94°C for 1 min, and then a final extension cycle at 58–62°C for 2 min, 74°C for 2 min. Aliquots of the resulting PCR products were separated on a 1% agarose gel and visualized with ethidium bromide. The remaining products were then purified using Magic PCR Preps (Promega Corp., Madison, WI) to remove unincorporated NTPs and sequenced directly using γ-^{32}P-labeled primers and the *fmol* DNA sequencing kit according to the manufacturer's instructions (Promega Corp., Madison, WI).

Motility and Microtubule-binding Assays

Wild-type or *sup-pf-1-1* dynein extracts were prepared by incubation of isolated axonemes in 10 mM MgATP in HMEEK buffer for 30 min followed by centrifugation for 20 min at 39,000 g. This protocol enhances the extraction of the outer dynein arms relative to the inner dynein arms (Goodenough and Heuser, 1984; Porter, M., unpublished observations). The extracts were then tested for their ability to support microtubule gliding in a perfusion assay as described by Vale and Toyoshima (1988). 5–10 μl were absorbed to a glass coverslip for 1–2 min, rinsed in buffer containing 1 mg/ml BSA, and then perfused with a solution containing 10–20 μg/ml taxol-stabilized brain microtubules and 1 mM MgATP. Dynein-induced translocation of taxol-stabilized microtubules was visualized by video-enhanced differential interference contrast microscopy as described by Porter et al. (1987). Microtubule binding activity was assayed by the addition of 10 μl of 2 mg/ml taxol-stabilized brain microtubules to 40 μl of dynein extract and incubation at room temperature for ~30 min. Samples that showed evidence of microtubule bundling by dark-field light microscopy were then diluted 10-fold, applied to carbon- and Formvar-coated coverslips, and negatively stained as described by Porter and Johnson (1983). Specimens were examined at a magnification of 39,000–55,000 on an electron microscope (CM10; Phillips Electronic Instruments Co., Mahway, NJ) operating at 80 kV. Axoneme sliding disintegration experiments were performed as described by Smith and Sale (1992).

Results

Relationship between sup-pf-1 and oda4 Mutations

sup-pf-1-1 and *oda4* are two closely linked outer arm muta-

tions (Luck and Piperno, 1989). *oda4* flagella lack the outer dynein arms and beat at approximately one third of the wild-type frequency, whereas *sup-pf-1* flagella retain the outer arm and beat at approximately half of the wild-type frequency (Brokaw and Kamiya, 1987). To determine if *sup-pf-1-1* and *oda4* represent two classes of mutant alleles within the same locus, we performed complementation tests in stable diploid cells. Diploid cells are more reliable than dikaryons for analyzing the relationship between different outer arm mutations because the resulting phenotypes are not affected by the presence or absence of preassembled outer arm complexes (see Luck and Piperno, 1989). As shown in Table II, *oda4/sup-pf-1-1* strains swim at *sup-pf-1-1* speeds, and their axonemes contain only the *sup-pf-1-1* form of the β-DHC. *oda4/ODA4+* diploid cells swim at wild-type speeds, and their axonemes contain the wild-type form of the β-DHC. The *oda4* mutation is therefore recessive to both wild-type and *sup-pf-1-1* alleles (Table II). In contrast, the *sup-pf-1-1* mutation is codominant with respect to wild-type, as has been reported previously in dikaryons (Huang et al., 1982). *sup-pf-1-1/ODA4+* cells swim faster than homozygous *sup-pf-1-1* strains and slower than wild-type cells, and both wild-type and mutant forms of the β-DHC assemble into the flagellar axonemes. Because the intermediate swimming phenotype can be difficult to score, we also analyzed the suppressor phenotype in diploid strains that are homozygous for the paralyzed central pair mutation *pf6*. Restoration of flagellar motility is intermediate in *sup-pf-1-1 pf6/ODA4+ pf6* diploids (Table II). However, the *sup-pf-1-1 pf6/oda4 pf6* diploids swim as well as the *sup-pf-1-1 pf6* homozygote (Table II). The recessive and codominant properties of *oda4* and *sup-pf-1-1* indicate that these alleles represent two distinct types of mutations occurring within the same gene. These properties also facilitate the identification of new *sup-pf-1* alleles (see below).

Both *sup-pf-1-1* and *oda4* mutations reduce the flagellar beat frequency (Brokaw and Kamiya, 1987), but the *sup-pf-1-1* mutation also restores motility to radial spoke and central pair defective strains (Huang et al., 1982). To examine whether the restoration of motility is simply the result of a decrease in outer arm activity or a β-DHC modification specific to the *sup-pf-1-1* mutation, we constructed a series of double-mutant strains containing other mutant dynein alleles in combination with the central pair mutation *pf6* (Table II). Suppression of flagellar paralysis was only observed with *sup-pf-1*, and not with any other outer dynein arm mutations tested. These data argue that the mechanism of suppression is not based on a loss of dynein function, but rather due to a specific change in dynein activity.

Linkage of the SUP-PF-1 Locus with a β-Dynein Clone

We have used RFLP analysis to place the β-DHC structural

Table II. Complementation and Suppression Tests

Genotype	Swimming phenotype	Outer arm phenotype (β-DHC phenotype)
Diploid strains:		
oda4 / +	Wild type	Outer arms present (β)
oda4 / *sup-pf-1-1*	Slow swimming	Outer arms present (β′)
sup-pf-1-1 / +	Intermediate speed	Outer arms present (β+β′)
+ *pf6* / + *pf6*	Twitch (*pf6*)	Outer arms present (β)
oda4 *pf6* / + *pf6*	Twitch (*pf6*)	Outer arms present (β)
sup-pf-1-1 *pf6* / + *pf6*	Partial suppression	Outer arms present (β+β′)
sup-pf-1-1 *pf6* / *sup-pf-1-1* *pf6*	Wobble (suppressed)	Outer arms present (β′)
oda4 *pf6* / *sup-pf-1-1* *pf6*	Wobble (suppressed)	Outer arms present (β′)
Haploid strains:		
pf6	Twitch	Outer arms present (β)
pf28 pf6	Short, paralyzed flagella	Outer arms missing
oda4 pf6	Short, paralyzed flagella	Outer arms missing
oda11 pf6	Twitch	Outer arms present, α-DHC missing
sup-pf-1-1 pf6	Wobble (suppressed)	Outer arms present (β′)

gene <1.2 centimorgans (cM) from the *SUP-PF-1* locus. In a previous study, a fragment of the β-DHC gene (*Dbl*) had been mapped to the left arm of linkage group IX, ~25 cM distal to the drug resistance marker *sr-1* (Ranum et al., 1988). These data placed the β-DHC gene ~8 cM (or roughly 800 kb) from the estimated position of the *SUP-PF-1* locus. Although the exact relationship between genetic map distance and DNA sequence in kilobases is not known, recent estimates are on the order of 50–100 kb/cM (Harris, 1989; Ferris and Goodenough, 1994). To analyze linkage more precisely, we examined the cosegregation of the *Dbl* clone and the *sup-pf-1-1* mutation directly. HinfI digests of *C. reinhardtii* and *C. smithii* DNA samples generate a RFLP in the β-DHC gene that can be detected by the *Dbl* clone (see Materials and Methods). We followed the segregation of this *Dbl* RFLP in the tetrad progeny of a cross between *C. smithii* and a strain of *C. reinhardtii* carrying both the mutant *sup-pf-1-1* allele and the *sr-1* marker. As shown in Fig. 1, the *C. reinhardtii* RFLPs recognized by the *Dbl* clone always cosegregated with the *sup-pf-1-1* motility phenotype. We have analyzed the segregation of all three markers (*sup-pf-1-1, sr1*, and the *Dbl* RFLP pattern) in 117 progeny collected from 63 tetrads (Table III). Although *sup-pf-1-1/sr1* recombinant progeny were recovered at the expected frequency, we never observed a recombination event between the *C. reinhardtii* β-DHC gene and the *sup-pf-1-1* mutation. These data place the β-DHC gene <~100 kb from the *sup-pf-1-1* mutation, and they are consistent with the interpretation that the *sup-pf-1-1* mutation is a defect in the β-DHC structural gene.

Localization of the sup-pf-1 Defects in the β-DHC

To determine the approximate location of the *sup-pf-1* lesions within the β-DHC, we purified wild-type and mutant outer arm subunits and then subjected these complexes to photolytic and proteolytic cleavage procedures (see Fig. 2 *A*). SDS-PAGE analysis of *sup-pf-1-1* and *sup-pf-1-2* axonemes had previously demonstrated changes in the electrophoretic mobility of the β-DHCs, but the site of these defects had not been identified (Huang et al., 1982; Luck and Piperno, 1989). High salt extraction of *sup-pf-1* axonemes followed by sucrose density centrifugation yields two major peaks of MgATPase activity that sediment at the same positions as the ATPase peaks in wild-type dynein extracts. The 21S peak contains the α and β outer arm heavy chains and associated intermediate and light chain subunits (Piperno and Luck, 1979). The ATPase activity and polypeptide composition of the 21S peaks are unchanged in both the *sup-pf-1-1* and *sup-pf-1-2* dyneins (data not shown).

One-dimensional linear maps of the wild-type outer arm heavy chains have been constructed on the basis of their sensitivity to vanadate-mediated UV cleavage (reviewed in King

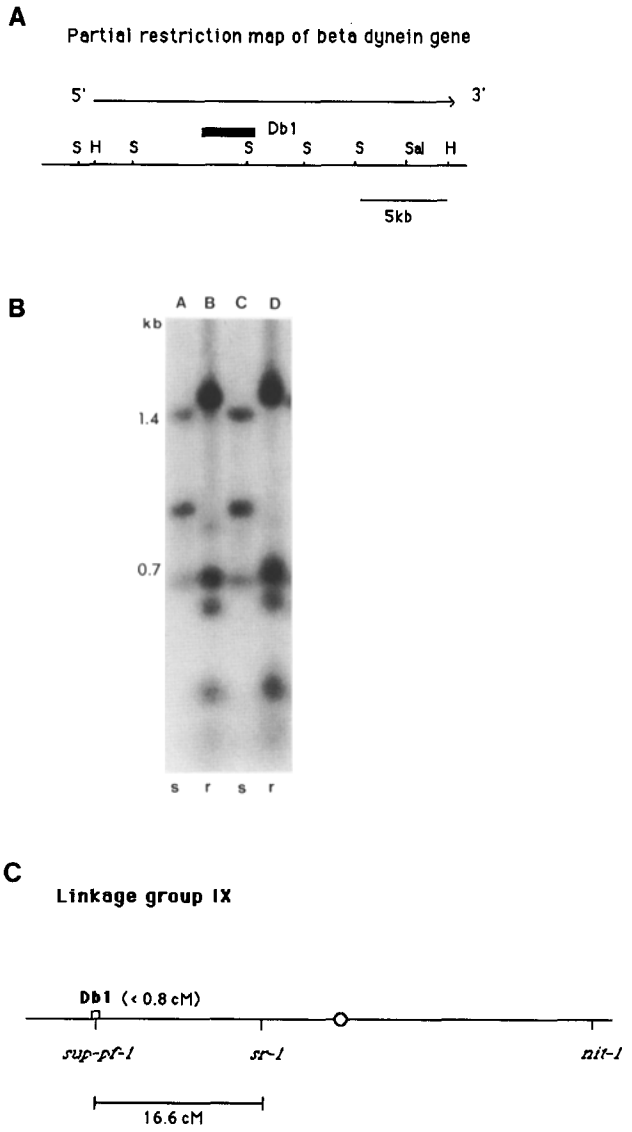

Figure 1. Cosegregation of the β-DHC gene with the *sup-pf-1* motility phenotype. (*A*) Restriction map of the β-DHC gene showing the position of the transcription unit and the 2.8-kb *Dbl* clone used as a hybridization probe (redrawn after Mitchell and Brown, 1994). (*B*) A Southern blot of DNA isolated from the four meiotic progeny (lanes *A–D*) of one tetrad of a cross between a *C. reinhardtii* strain carrying the *sup-pf-1* and *sr-1* markers and a wild-type *C. smithii* strain. The DNA was digested with *Hinf*I, separated on a 0.8% agarose gel, transferred to a Zetabind membrane, and probed with *Dbl*. The *C. reinhardtii* RFLP pattern (*r*) cosegregates with the *sup-pf-1* motility phenotype in progeny *B* and *D*, and the *C. smithii* RFLP pattern (*s*) cosegregates with the wild-type motility phenotype in progeny *A* and *C*. (*C*) Map of linkage group IX showing the positions of the genetic markers and their relationship to the β-DHC gene.

Table III. Cosegregation of the sup-pf-1 Motility Phenotype with the β-DHC Gene

Markers	Tetrad data (PD/NPD/TT)	Random progeny (recombinant/total)	Marker distance
			cM
Dbl vs *sup-pf-1-1*	18:0:0	0/45	<1.2
sr1 vs *sup-pf-1-1*	40:0:20		~16.6
Dbl vs *sr1*	11:0:7	11/45	~22.0

The cosegregation of the *Dbl* molecular marker with the *sup-pf-1* motility phenotype was examined in 18 complete tetrads and in single progeny of an additional 45 tetrads. *PD*, parental ditype; *NPD*, nonparental ditype; *TT*, tetratype. Map distance was determined using the equations $cM = TT/2(PD + NPD + TT)$ for complete tetrads and $cM = recombinant/total$ progeny for random progeny. Tetrad and random progeny data were combined using the equation $cM = (TT + recombinant)/[2(PD + NPD + TT) + total]$.

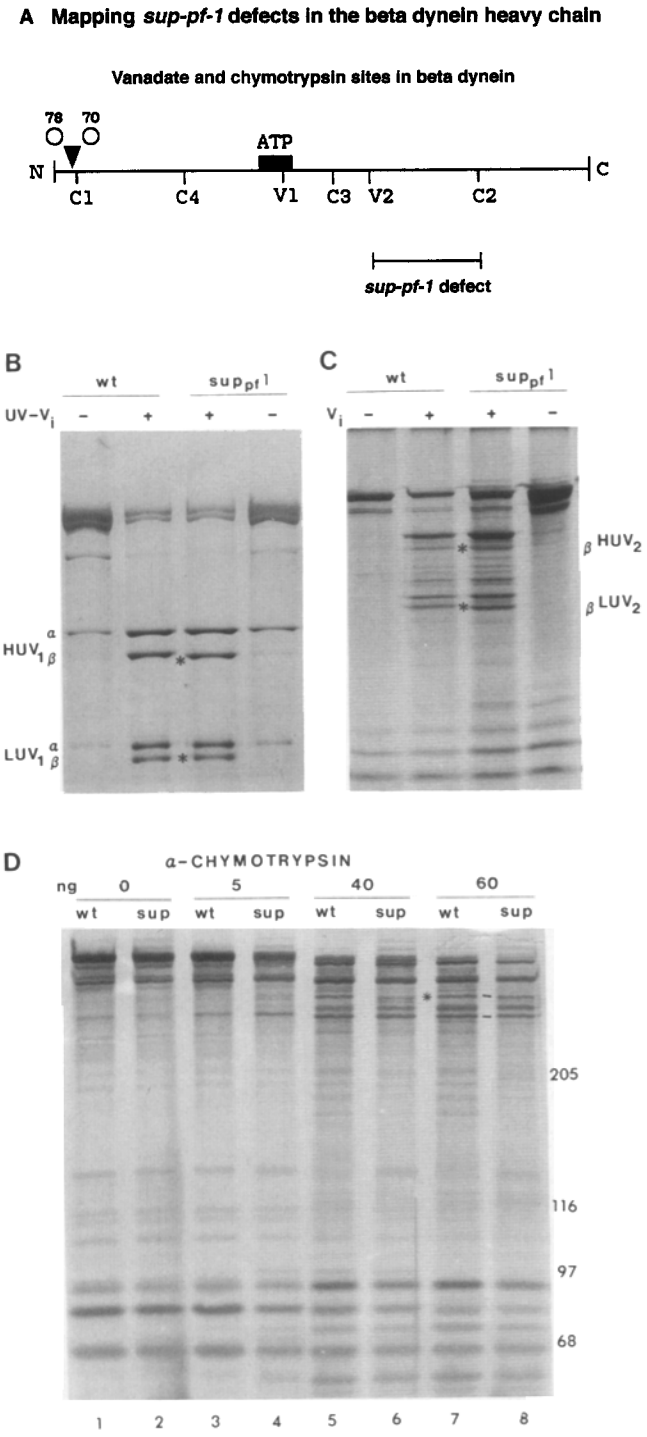

Figure 2. Localization of the *sup-pf-1* defect in the β-DHC. (*A*) Revised map of the β-DHC and strategy for mapping *sup-pf-1* defects. The positions of the amino and carboxy termini, the V1 and V2 cleavage sites, and the chymotrypsin-sensitive sites are shown here (redrawn after King and Witman, 1987, 1988; Mitchell and Brown, 1994). The proposed ATP and intermediate chain-binding sites are also indicated. (*B*) SDS-PAGE patterns of wild-type and *sup-pf-1* dyneins after V1 cleavage. The top portion of a silver-stained, 3.2–5% acrylamide, 0–2-M urea gradient gel (Neville, 1971) is shown here. Purified 21S αβ dynein subunits from wild-type (first two lanes) and *sup-pf-1-1* (last two lanes) strains were subjected to UV irradiation in the absence (−) and presence (+) of MgATP and 100 μM vanadate to generate two HUV-1 and two LUV-1 polypeptide fragments. The heavy chain origin of each of these fragments is indicated on the left. The bands marked with asterisks are the β-DHC fragments. (*C*) SDS-PAGE patterns of wild-type and *sup-pf-1* dyneins after V2 cleavage. The top portion of a silver-stained, 5–15% acrylamide, 0–2.4-M glycerol gradient gel is shown here. Purified 20S αβ dynein subunits from *pf9-2* (first two lanes) and *pf9-2 sup-pf-1-1* (last two lanes) strains were subjected to UV irradiation in the absence (−) and presence (+) of $MnSO_4$ and 0.5 mM vanadate to generate multiple HUV-2 and LUV-2 fragments. The positions of the β-DHC V2 fragments (bands marked with asterisks) are indicated on the right. (*D*) SDS-PAGE pattern of wild-type and *sup-pf-1* dyneins after digestion with α-chymotrypsin. The top portion of a silver-stained 5–10% acrylamide gradient gel is shown here. 1.5 μg of purified 20S αβ dynein subunits from wild-type (*wt*) and *sup-pf-1-1* (*sup*) strains were incubated with increasing amounts of the proteolytic enzyme α-chymotrypsin. The band marked with an asterisk in lane 7 corresponds to the ~348-kd fragment of the wild-type β-DHC. The position of this band is shifted slightly in the *sup-pf-1-1* sample (lane 8, *tilted bar*). The positions of the molecular weight markers are indicated on the right.

and Witman, 1987, 1988). UV irradiation of the wild-type αβ complex in the presence of MgATP and vanadate (V1 cleavage) is thought to cut both DHCs at their primary ATP binding site (Fig. 2 *A*). V1 cleavage generates four polypeptide fragments; one pair of fragments derived from the α-DHC at ~290 and ~190 kD, and a second pair derived from the β-DHC at ~255 and ~185 kD (King and Witman, 1987). As shown in Fig. 2 *B*, V1 cleavage of the *sup-pf-1-1* α/β DHCs also generates four polypeptide fragments. Three of these fragments comigrate with their wild-type counterparts, but one fragment derived from the β-DHC (HUV-1) is consistently smaller in the *sup-pf-1-1* dynein ($n = 4$ independent preparations). Identical results have been observed with the *sup-pf-1-2* β-DHC ($n = 4$ independent preparations). These data indicate that the *sup-pf-1* mutations are located in a region carboxy-terminal to the predicted ATP binding site.

The DHCs contain three other putative nucleotide binding sites of unknown significance (Gibbons et al., 1991; Ogawa, 1991; Mitchell and Brown, 1994). To determine if the *sup-pf-1* mutations might alter one of these sites and to further localize the site of the *sup-pf-1* defects within the β-DHC, we compared the wild-type and *sup-pf-1* dyneins after V2 cleavage. UV irradiation of wild-type αβ subunits in the presence of Mn^{2+} and vanadate cuts the DHCs at several sites and generates multiple polypeptide fragments. Three pairs of cleavage products are derived from the α-DHC and one pair from the β-DHC (King and Witman, 1987; Fig. 2 *C*). V2 cleavage of the *sup-pf-1* αβ subunits generates a similar pattern of polypeptide fragments, but only one fragment is shifted relative to its wild-type counterpart: the smallest LUV-2 fragment derived from the β-DHC (Fig. 2 *C*). This shift corresponds to an apparent decrease of ~2–3 kD in both the *sup-pf-1-1* and the *sup-pf-1-2* DHCs ($n = 8$ independent experiments). The *sup-pf-1* defects therefore reside in a region carboxy-terminal to all four proposed nucleotide-binding sites.

Further localization of the *sup-pf-1* defects within the carboxy terminal LUV2 fragment was pursued using limited proteolysis. Partial digestion with α-chymotrypsin cleaves the β-DHC into multiple polypeptide fragments (King and

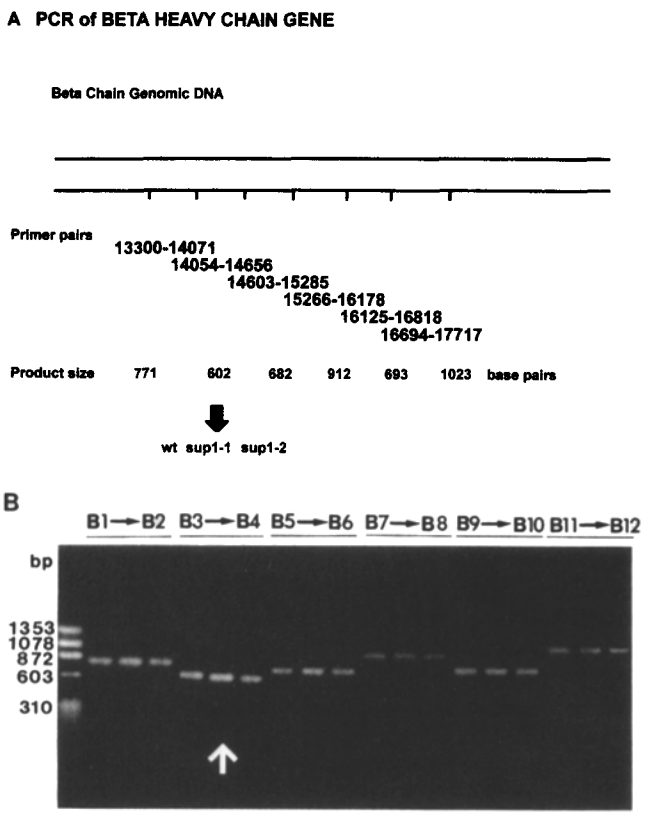

Figure 3. PCR strategy for the identification of *sup-pf-1* defects. (*A*) Schematic diagram of the ~5-kb portion of genomic DNA encoding the β-DHC between the V2 and C2 cleavage sites. The positions of the oligonucleotide primers and the expected PCR product sizes are indicated. (*B*) Agarose gel profile of PCR products. The PCR products obtained with each primer pair are shown for wild-type, *sup-pf-1-1*, and *sup-pf-1-2* DNA samples, respectively, on a 1% agarose gel stained with ethidium bromide.

Witman, 1988). The initial site of cleavage (the C1 site) is ~10 kD from the amino terminus, but the next site (the C2 site) is ~80 kD from the carboxy terminus (King and Witman, 1988; see Fig. 2 *A*). Cleavage at the C2 site therefore generates β-DHC fragments of ~348 and ~82 kD (King and Witman, 1988). We examined several limited digests of wild-type and *sup-pf-1-1* dyneins, and although we routinely observed proteolytic digestion products in vicinity of 82 kD, we never observed a difference between wild-type and *sup-pf-1-1* digestion products in this region (n = 5 experiments) (see Fig. 2 *D*). However, we were sometimes able to resolve small differences in the higher molecular weight digestion products (~345 kD) (see Fig. 2 *D*, lanes *7* and *8*). Similar results were obtained with the *sup-pf-1-2* samples. These data suggested that the *sup-pf-1* defects are contained within the ~100-kD region between the V2 site and the C2 site.

Identification of the sup-pf-1 Defects in the β-DHC Gene

We have identified the DNA sequence defects in the *sup-pf-1-1* and *sup-pf-1-2* mutations (Fig. 3 and 4). Six pairs of oligonucleotide primers were designed that span the ~5-kb of genomic DNA encoding the region between the V2 and C2 cleavage sites (see Mitchell and Brown, 1994, and Fig. 3 *A*). These primers were used to amplify small (600–1000 bp) portions of the β-DHC gene from wild-type and mutant DNA by PCR. Analysis of the resulting PCR products by agarose gel electrophoresis identified one set of products that was consistently smaller in both the *sup-pf-1-1* and the *sup-pf-1-2* DNA samples (see Fig. 3 *B*).

Direct sequencing of the PCR products reveals the presence of a 21-bp in-frame deletion in the *sup-pf-1-1* DNA and a different 30-bp in-frame deletion in the *sup-pf-1-2* DNA. These same sequence defects were observed in multiple independent PCR reactions and in several *sup-pf-1-1* progeny.

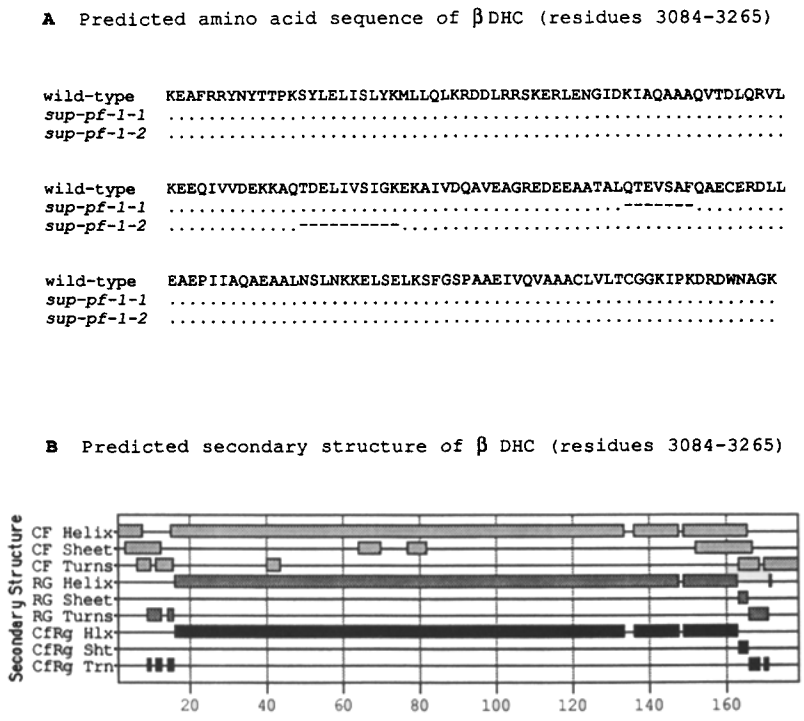

Figure 4. Predicted amino acid sequence and secondary structure in *sup-pf-1* alleles. (*A*) The predicted amino acid sequence of the wild-type β-DHC (amino acids 3084-3265) is shown on the top line. The identical amino acids in the mutant sequences are indicated by periods on the lines below. The *sup-pf-1-1* mutation results in a 7-amino acid deletion and the *sup-pf-1-2* mutation in a 10-amino acid deletion. (*B*) Predicted secondary structure of *sup-pf-1* region in the β-DHC. The region corresponding to amino acids 3084 to 3265 in the wild-type *C. reinhardtii* β-DHC was analyzed using the secondary structure predictions of Chou and Fasman (1978) and Garnier et al. (1978) available on the MacVector software package. *CF*, Chou and Fasman; *RG*, Robson and Garnier; *CfRg*, combined Chou and Fasman and Robson and Garnier.

Control experiments confirmed that neither one of these sequence defects is present in the DNA of the parental strain *pf6* from which these two *sup-pf-1* alleles were isolated (Luck and Piperno, 1989). The change in the predicted amino acid sequence of the β-DHC corresponds to a deletion of amino acids 3190-3196 in the *sup-pf-1-1* allele and a deletion of amino acids 3158-3167 in the *sup-pf-1-2* allele (see Fig. 4 *A*). These deletions should decrease the apparent size of the β-DHC by ~733 and ~1056 D, respectively. These decreases are only slightly smaller than those estimated by SDS-PAGE of the V2 cleavage products (see above).

We have used several computer programs that predict secondary structure to determine if the *sup-pf-1* mutations fall within a well-defined polypeptide domain (Chou and Fasman, 1978; Garnier et al., 1978; Lupas et al., 1991). Amino acids 3099-3249 are predicted to form a relatively short, α-helical domain that would be decreased by one turn in the *sup-pf-1-1* allele and one and a half turns in the *sup-pf-1-2* allele (see Fig. 4 *B*). The amino acid sequence predicted to form this domain is conserved in nearly all DHCs that have been sequenced thus far (e.g., ~45% sequence identity with the sea urchin β-DHC, see Gibbons et al., 1991; Ogawa, 1991). Although the actual structure formed by these amino acids cannot be determined by simple inspection of the primary sequence, it is striking that this region is one of the few α-helical, coiled-coil domains predicted in nearly all of the axonemal and cytoplasmic DHC sequences (Lupas et al., 1991; see discussion in Mitchell and Brown, 1994; Li et al., 1994).

Isolation and Characterization of Additional sup-pf-1 Alleles

The identification of *sup-pf-1* mutant defects to the same region in two different alleles indicates that this domain plays a role in the regulation of β-DHC activity, but does not preclude the possibility that changes in other domains of the β-DHC may also restore flagellar motility to radial spoke– and central pair defective–strains. We therefore isolated and analyzed additional suppressor mutations to address this question. Two mutations (*RR5* and *RR48*) were isolated in a screen for suppressors of the central pair mutation *pf16BR3* (Dutcher et al., 1984; Porter et al., 1992), and one allele (*RI3*) was obtained previously as an extragenic suppressor of *pf6* (Luck and Piperno, 1989). In a wild-type background, each of these mutations has a distinctive slow-swimming phenotype, but no alteration in the β-DHC has been observed by SDS-PAGE of isolated axonemes. Complementation tests with *oda4* have confirmed that these suppressors are new alleles at the *SUP-PF-1/ODA4* locus (Table IV). However, recombination analysis has indicated that it is possible to isolate intragenic recombinants between some of these alleles (Table IV). In pairwise crosses between different strains, the *sup-pf-1-1* and *oda4* alleles failed to recombine with either the *RR5* or the *RR48* mutation, but recombination was observed between the *RR5 and RR48* alleles. Mutations in more than one domain of the β-DHC can therefore alter both the flagellar beat frequency and suppress flagellar paralysis (Table V). Since the β-DHC gene spans ~20 kb of genomic DNA (Mitchell and Brown, 1994), these data also provide a new estimate of <22 kb/cM for the relationship between physical and genetic map distances at the *SUP-PF-1* locus.

Microtubule Binding and Motility Properties of the sup-pf-1 Dyneins

Because the *sup-pf-1* mutations have such dramatic effects on both the flagellar beat frequency and forward swimming velocity (Table V), it has been proposed that certain parameters of the microtubule cross-bridge cycle may be altered in *sup-pf-1* dyneins (Brokaw and Kamiya, 1987). To address

Table IV. Identification of New sup-pf-1 Alleles

Recombination tests*	Segregation (PD/NPD/TT)	Map distance
sup-pf-1-1 × *RR5*	107:0:0	<0.5 cM
sup-pf-1-1 × *RR48*	86:0:0	<0.6 cM
oda4 × *RR5*	44:0:0	<1.0 cM
oda4 × *RR48*	169:0:0	<0.3 cM
RR5 × *RR48*	273:0:5	~0.9 cM
RR5 RR48 × *wild-type*	57:0:1	~0.9 cM
Complementation tests	**Motility phenotype**	**Conclusions**
RR5 / + over *pf6* / *pf6*	Partial suppression	*RR5* is codominant
RR48 / + over *pf6* / *pf6*	Partial suppression	*RR48* is codominant
oda4 / *RR5* over *pf6* / *pf6*	Suppressed *pf6*	Alleles at the same locus
oda4 / *RR48* over *pf6* / *pf6*	Suppressed *pf6*	Alleles at the same locus

* All crosses were homozygous for the *pf6* mutation. The *oda4 pf6* strain assembles short, immotile flagella, and it is easily distinguished from both *pf6* and *sup-pf-1 pf6*. No recombinants were previously observed between *sup-pf-1-1* and *oda4* in 60 tetrads (Luck and Piperno, 1989). *PD*, parental ditype, *NPD*, nonparental ditype, *TT*, tetratype.

Table V. Motility of Dynein Mutants

Strain	Beat frequency	Swimming velocity	Sliding velocity
	Hz (n)	*μm/s (n)*	*μm/s (n)*
wild-type	59.4 ± 3.9 (20)	152 ± 23 (25)	6.1 ± 2.5 (14)
sup-pf-1-1 (R6)	29.1 ± 2.4 (20)	72 ± 10 (25)	6.7 ± 2.8 (27)
sup-pf-1-2 (D22)	15.5 ± 1.2 (20)	53 ± 9 (30)	ND
sup-pf-1-3 (R13)	45.6 ± 2.1 (20)	88 ± 8 (30)	ND
sup-pf-1-4 (RR5)	45.5 ± 3.4 (20)	76 ± 9 (30)	ND
sup-pf-1-5 (RR48)	33.0 ± 2.9 (20)	70 ± 10 (30)	ND
pf9-2	52.0 ± 5.7 (20)	64 ± 10 (19)	9.1 ± 2.9 (41)
sup-pf-1-1 pf9-2	24.9 ± 1.0 (20)	42 ± 7 (30)	2.3 ± 1.2 (20)

Beat frequencies, swimming velocities, and sliding velocities are expressed as mean ± SD (*n*, sample size). Axoneme sliding velocities were determined by Elizabeth Smith (Emory University, Atlanta, GA, and University of Minnesota, St. Paul, MN) using a NaCl buffer as described by Smith and Sale (1992).

this question, we analyzed several characteristics of the *sup-pf-1* dyneins in vitro, including microtubule binding and microtubule translocation activity. Our experiments indicated that crude extracts of *sup-pf-1* dyneins can bind and cross-bridge purified brain microtubules into large bundles visible by both dark-field light microscopy and negative-stain transmission electron microscopy. Negatively stained images of the *sup-pf-1-1* dynein–microtubule complexes revealed the presence of dynein cross-bridges occurring with a 24-nm periodicity characteristic of wild-type dynein cross-bridges (Fig. 5). Microtubule binding activity is therefore apparently unaltered in the *sup-pf-1* dyneins. Similarly, *sup-pf-1-1* dynein extracts support microtubule gliding activity in vitro, and *sup-pf-1-1* axonemes also undergo sliding disintegration at nearly wild-type velocities (Table V, and Smith and Sale, 1992). These results indicate that the activity of the outer dynein arm is not grossly disrupted in *sup-pf-1* strains.

However, under certain experimental conditions, the activity of the *sup-pf-1-1* dyneins can be clearly distinguished from wild-type. In particular, dramatic effects on microtubule sliding velocities can be observed in double-mutant strains. As shown in Table V, *pf9-2* axonemes, which lack the I1 inner arm subunits, undergo sliding disintegration at rates greater than or equal to wild-type axonemes, but axonemes from the double-mutant *pf9-2 sup-pf-1-1* undergo sliding disintegration at velocities significantly below that of either *pf9-2* or *sup-pf-1-1* alone. Similar results have been observed with the α-DHC mutant *oda11* (Kurimoto, E., and R. Kamiya, personal communication). *Oda11* axonemes undergo sliding disintegration at near wild-type velocities, but *oda11 sup-pf-1-1* axonemes slide apart at approximately half of the wild-type rates (Kurimoto, E., and R. Kamiya, personal communication). Such synergistic defects indicate that interactions between the multiple dynein isoforms are altered in the *sup-pf-1* strains.

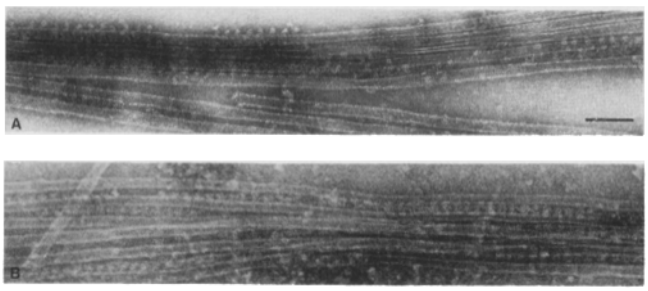

Figure 5. Dynein decoration of taxol-stabilized microtubules. Wild-type and *sup-pf-1* dynein extracts were incubated with repolymerized, taxol-stabilized microtubules, negatively stained with uranyl acetate, and imaged by transmission EM. (*A*) Wild-type dynein-decorated microtubules. (*B*) *sup-pf-1* dynein–decorated microtubules. Note periodic cross-bridges. Bar, 0.1 μm.

Discussion

Mutations in the β-DHC Locus

In this study, we report four lines of evidence that identify the *sup-pf-1* mutations as mutant β-DHC alleles. First, recombination analysis has shown that the *sup-pf-1* alleles and *oda4* alleles are tightly linked genetically (Table IV). Second, complementation tests indicate that *sup-pf-1* and *oda4* represent two different types of mutant alleles within the same locus (Table II). Both the biochemical and motility phenotypes of the *sup-pf-1* mutations are dominant with respect to *oda4* alleles and codominant with respect to wild-type alleles (Huang et al., 1982, and this study, Tables II and IV). Third, RFLP analysis with a β-DHC genomic probe demonstrates that the *sup-pf-1* mutation is tightly linked to the β-DHC gene (Fig. 1 and Table III). Finally, the biochemical and sequence analyses of two *sup-pf-1* alleles have revealed the sites of the mutant lesions within the β-DHC (Figures 2–4). The DNA sequence defects are both in-frame deletions that would result in relatively small decreases (~700–1000 D) in predicted molecular mass of the β-DHC. These changes are consistent with the observed shifts in electrophoretic mobilities shown in Fig. 2. Independent evidence in support of our conclusions comes from the recent characterization of a novel *oda4* mutation, the *oda4-s7* allele, which results in the assembly of an outer arm dynein containing a truncated form of the β-DHC (Sakakibara et al., 1993). Taken together, the data indicate that the *SUP-PF-1/ODA4* locus is the β-DHC structural gene. The *sup-pf-1* mutations are the first DHC mutations to be characterized at the DNA sequence level.

Although mutations in any of 13 different loci can disrupt the assembly of the outer dynein arm (Huang et al., 1979; Kamiya, 1988; Sakakibara et al., 1991), the frequency with which mutations appear at the *SUP-PF-1/ODA4* locus is strik-

ing. More than 16 different *oda4* alleles have been isolated (Kamiya, 1988), as well as five independent *sup-pf-1* alleles (Luck and Piperno, 1989, and this study). This sensitivity may be a reflection of the fact that the β-DHC gene represents a relatively large target (>20 kb) for mutagenesis. However, the *ODA2/PF28* locus, which may encode the γ-DHC (Wilkerson et al., 1994), is represented by only five mutant alleles (Mitchell and Rosenbaum, 1984; Kamiya, 1988). Likewise, the α-DHC locus is represented by the single *oda11* mutation, which only blocks the assembly of the α-DHC and an associated 16-kD light chain (Sakakibara et al., 1991). Although it remains a possibility that additional alleles at these loci may suppress flagellar paralysis and/or completely block outer arm assembly, the current data suggest that the β-DHC plays a more central role in both outer arm assembly and function (Sakakibara et al., 1991). The future sequence analysis of the *oda4* alleles could therefore provide additional insights into other functional domains in the β-DHC. For example, studies with the *oda4-s7* mutant strain have suggested that the NH_2-terminal third of the β-DHC is sufficient to support the stable assembly of the other outer arm subunits onto the flagellar axoneme, but insufficient to either generate force or suppress flagellar paralysis (Sakakibara et al., 1993). Although the actual molecular lesion in the *oda4-s7* allele has not yet been identified, biochemical observations are consistent with the model in which the NH_2-terminal domain (~160 kD) of the β-DHC functions as an adaptor that interacts with the other heavy, intermediate, and light chain polypeptides to form the A-tubule binding site. The central region of the DHC that contains the multiple nucleotide-binding sites may form the globular head or motor domain (Mocz and Gibbons, 1993; Sakakibara et al., 1993; Mitchell and Brown, 1994; see Fig. 6). Further characterization of the NH_2-terminal region by sequence analysis of *oda4* alleles and by transformation with NH_2-terminal constructs could therefore define the β-DHC domains involved in subunit binding and outer arm assembly.

Location of sup-pf-1 Mutations

Our studies with the *sup-pf-1* mutations indicate that small deletions in a predicted coiled-coil domain downstream of the last nucleotide-binding site can have dramatic effects on flagellar motility (Figs. 4 and 6). In addition, the location and size of this coiled-coil domain have been conserved in nearly all axonemal and cytoplasmic DHC sequences reported thus far (see Mitchell and Brown, 1994; Li et al., 1994, for comparisons). These observations indicate that this domain probably performs a conserved function in the structural organization of the dynein complex. Scanning transmission EM has demonstrated that both axonemal and cytoplasmic dyneins contain two or three large, globular heads (~350 kD each) that are attached by slender stalks to a common base (Witman et al., 1983; Vallee et al., 1988). Since the NH_2-terminal 160 kD of the β-DHC appears to be contained within the stalk (Sakakibara et al., 1993), it seems likely that the remainder of the DHC, including the coiled-coil domain, is located in or near the globular dynein head, but the exact location of this domain remains unknown. Others have suggested that this coiled-coil domain may be important in the formation of a small stalk, the B-link structure, which projects from the globular head and attaches it to a B-subfiber microtubule (Gibbons et al., 1991; Asai and Brokaw, 1993; Goodenough and Heuser, 1989). Another proposal is that this coiled-coil domain may lie outside the motor domain and instead plays a role in DHC interactions (Mikami et al., 1993; Holzbaur et al., 1994). A third possibility is that this coiled-coil domain plays a role in the conformational changes associated with force production. The latter could be analogous to the α-helical "neck" domain located within the myosin S1 head that is thought to function as a lever during the myosin cross-bridge cycle (Uyeda and Spudich, 1993). Clearly, further insight into the precise function of the coiled-coil domain will require additional information on the three-dimensional organization of the DHC. In addition, the sequence analysis of the other *sup-pf-1* alleles should reveal the location of related regulatory domains within the β-DHC.

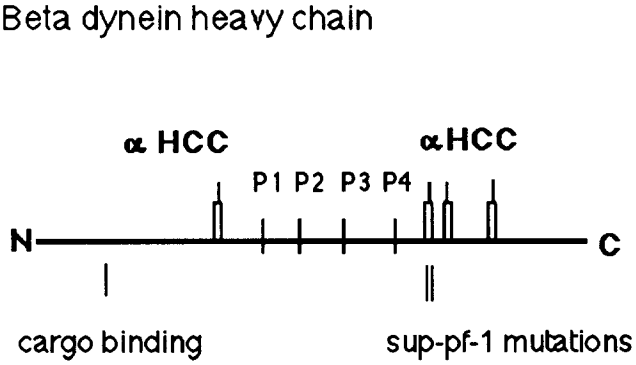

Figure 6. Diagram of functional domains in the β-DHC. The position of the *sup-pf-1-1* and *sup-pf-1-2* mutations is indicated with respect to the location of other domains of the β-DHC. The four nucleotide-binding sites or P-loops (*P1–P4*) as well as the four α-helical coiled-coil domains (*α-HCC*) are based on the sequence analysis of Mitchell and Brown (1994). The location of the cargo-binding site or axoneme-binding site is based on the analysis of the *oda4-s7* strain (Sakakibara et al., 1993).

It is interesting to note other examples of sequence changes that alter motor velocities. First, a second class of mutations that alter the flagellar beat frequency has been identified in the structural gene for the 70-kD intermediate chain (Mitchell and Kang, 1993). The 70-kD subunit has been localized to the base of the outer dynein arm by immunoelectron microscopy (King and Witman, 1990), and it is thought to play a role in dynein attachment to the A-tubule (Mitchell and Kang, 1991, 1993). Reversion analysis of the 70-kD intermediate chain has identified a subset of mutations within the structural gene that allow normal outer arm assembly, but inhibit outer arm function. These studies suggest that cooperative interactions between outer arm subunits may be an essential component in the effective coupling of outer arm activity to increases in flagellar beat frequency (Mitchell and Kang, 1993). Second, in *Drosophila* muscle tissue, two myosin heavy chain isoforms have been identified that differ solely in the sequence of a single exon encoding segments of the hinge region between the myosin S-2 domain and the light meromyosin rod domain (Collier et al., 1990). The tissue distribution of these two isoforms can be correlated with differences in muscle contraction speed. Finally, in vitro motility assays using recombinant kinesin and kinesin-like proteins have demonstrated that changes in the

length of the tail domain can have significant effects on microtubule translocation velocities (Chandra et al., 1993*a*, 1993*b*; Stewart et al., 1993). These studies suggest that the geometry of a motor domain with respect to its filament substrate can strongly influence its activity.

Biochemical Properties of the sup-pf-1 Dyneins

The earliest studies on the *sup-pf-1-1* mutation suggested that the outer arm dyneins might be nonfunctional in *sup-pf-1-1* cells because the flagellar beat frequency is approximately one half that of wild-type cells (Brokaw et al., 1982). More recent work has shown that *sup-pf-1-1* strains are more active than either *oda4* strains, which lack the outer arm (Brokaw and Kamiya, 1987), or *oda4-s7* strains, which lack the β-DHC ATP hydrolytic site (Sakakibara et al., 1993). The outer arm dyneins in the *sup-pf-1-1* strains must, therefore, retain at least some force producing activity. In addition, quantitative analysis of outer arm structure by image-averaging procedures has indicated that *sup-pf-1-1* outer arms are indistinguishable from wild-type (Mastronarde et al., 1992). Our studies with the purified *sup-pf-1-1* dyneins in vitro have demonstrated that both the ATP-binding and microtubule-binding activities of the outer dynein arm are apparently normal (see Figs. 2 and 6). Microtubule gliding and axoneme sliding velocities are also essentially wild-type (Table V, and Smith and Sale, 1992). However, decreases in axoneme sliding velocities have been observed in two different *sup-pf-1* recombinant strains (Table V and Kurimoto and Kamiya, personal communication). In both the *pf9-2 sup-pf-1-1* and *oda11 sup-pf-1-1* double mutants, axoneme sliding velocities decrease significantly below that observed with either mutant alone. Taken together, these observations suggest that the *sup-pf-1* defect does not directly affect the dynein cross-bridge cycle in vitro, but instead, it alters a feedback mechanism that normally coordinates the activities of the multiple dynein motors in situ.

Mechanism of Suppression and Relationship to Other Suppressor Loci

Recent studies have provided new insights into the mechanism by which changes in β-DHC activity could lead to the restoration of flagellar motility. First, in vitro motility assays have indicated that the inner and outer dynein arms drive microtubule translocation at significantly different intrinsic speeds (Kurimoto and Kamiya, 1991; Kamiya et al., 1989). To work together efficiently, these different dynein isoforms must be selectively activated and inhibited at different points in the flagellar beat cycle. This may involve a mechanical feedback loop, such as the model of curvature control first proposed by Brokaw (1971), in which changes in microtubule spacing or the microtubule surface lattice may selectively activate or inhibit subsets of dynein arms. Alternatively, cooperative interactions between the dynein arms may modulate their activity, such that the outer arms are selectively inhibited, or the inner arms are selectively stimulated. A third possibility is that signals originating from the radial spoke/central pair complex serve to coordinate the activity of the multiple dynein motors.

Several lines of structural and genetic evidence implicate the central pair and radial spoke structures as key modulators of dynein arm activity (reviewed in Smith and Sale, 1994). Most recently, Smith and Sale (1992) have shown that microtubule sliding velocities are dramatically reduced in central pair– or radial spoke–defective axonemes. Their reconstitution experiments further suggest that these changes in sliding velocities may be mediated by posttranslational modification of the dyneins, and that both the inner and outer dynein arms could be targets of this regulatory machinery (Smith and Sale, 1992). These studies implicate the radial spokes as activators of dynein-driven microtubule sliding, but it is uncertain if the activating signal is acting on all the dynein isoforms or only a subset. In addition, it is also possible that radial spokes do not directly activate the dyneins, but instead, they act by modifying an inhibitory control system within the axoneme.

The presence of such an inhibitory control system has been suggested by the analysis of another group of extragenic suppressors that restore flagellar movement to radial spoke–defective strains (Huang et al., 1982). These strains (*pf2*, *pf3*, *sup-pf-3*, *sup-pf-4*, and *sup-pf-5*) share overlapping defects in a group of axonemal polypeptides known as the radial spoke–specific control system (Huang et al., 1982) or more recently as the "dynein regulatory complex" (DRC) (Piperno et al., 1992). The implication from these studies is that the suppressors are revealing sites of regulation in wild-type cells. We have recently localized components of this control system to the junction between the radial spokes and the inner and outer dynein arms (Mastronarde et al., 1992; Gardner, L., E. O'Toole, C. Perrone, T. Giddings, and M. Porter, manuscript in preparation). This complex is ideally positioned to mediate local signals, either mechanical, chemical, or both, between the radial spokes and the dynein arms. One model is that the central pair/radial spoke complex sends a signal to the DRC, turning the inhibitory control system off and thereby locally activating a subset of dynein arms (Huang et al., 1982; Smith and Sale, 1994). This signaling pathway need not necessarily work only in one direction, especially if cooperative interactions between different dynein isoforms provide mechanical feedback to the DRC.

By inference from the suppressor mutations, wild-type cells can regulate dynein activity in two ways: (*a*) by inactivating a part of the inhibitory control system (the DRC) or (*b*) by inactivating or adjusting the activity of a dynein isoform. The different classes of suppressors (e.g., DRC mutants, *pf9-2*, and *sup-pf-1*) are examples of these mechanisms. Furthermore, as suggested by the work of Smith and Sale (1992), adjustments of dynein activity may involve posttranslational modifications. Although the β-DHC itself is apparently not a target for phosphorylation (Luck and Piperno, 1989), it is possible that changes in β-DHC activity could lead to secondary modifications of other axonemal components. For example, since the *sup-pf-1* mutation can increase the sliding velocities of radial spoke defective axonemes (Smith and Sale, 1992), it would be worthwhile to examine the phosphorylation state of other polypeptides in *sup-pf-1* axonemes. This and the future study of the other suppressor loci should help to identify the regulatory mechanisms that coordinate dynein activity and generate flagellar motility.

The *pf16BR3* suppressors were isolated with the help of Zenta Ramanis while one of us (S. K. Dutcher) was a National Institutes of Health postdoctoral fellow in the laboratory of David Luck. M. E. Porter would like to

acknowledge David Luck for encouragement to pursue the analysis of these suppressors. M. E. Porter would also like to thank Elizabeth Smith for the measurement of axoneme sliding velocities, David Johnson for patient instruction, and members of the Porter Laboratory and Tom Hays for constructive comments on this manuscript. This work was supported by National Science Foundation grants (DCB8518224, DCB9005079, and DMB9023601) to M. E. Porter and S. K. Dutcher and a National Institutes of Health grant (GM44228) to D. R. Mitchell. Additional support to M. E. Porter was provided by start-up funds from the Graduate School of the University of Minnesota, the Minnesota Medical Foundation, the University of Minnesota's American Cancer Society Institutional Grant IN-30-28, and the McKnight-Land Grant Professorship. This work was also aided in part by a Basil O'Connor Starter Scholar Research Award no. 5-FY91-0607 from the March of Dimes Birth Defects Foundation.

Received for publication 18 May 1994 and in revised form 1 July 1994.

References

Asai, D. J., and C. J. Brokaw. 1993. Dynein heavy chain isoforms and axonemal motility. *Trends Cell Biol.* 3:398–402.

Bradford, M. 1976. A rapid and sensitive method for quantitation of microgram quantities of proteins utilizing the principle of protein-dye binding. *Anal. Biochem.* 72:248–284.

Brokaw, C. J., and R. Kamiya. 1987. Bending patterns of *Chlamydomonas* flagella. IV. Mutants with defects in inner and outer dynein arms indicate differences in dynein arm function. *Cell Motil. Cytoskel.* 8:68–75.

Brokaw, C. J., D. J. L. Luck, and B. Huang. 1982. Analysis of the movement of *Chlamydomonas* flagella: the function of the radial spoke system is revealed by comparison of wild type and mutant flagella. *J. Cell Biol.* 92:722–732.

Chandra, R., E. D. Salmon, H. P. Erickson, A. Lockhart, and S. A. Endow. 1993*a*. Structural and functional domains of the *Drosophila* ncd microtubule motor protein. *J. Biol. Chem.* 268:9005–9013.

Chandra, R., S. A. Endow, and E. D. Salmon. 1993*b*. An N-terminal truncation of the ncd motor protein supports diffusional movement of microtubules in motility assays. *J. Cell Sci.* 104:899–906.

Chou, P. Y., and G. D. Fasman. 1978. Empirical predictions of protein conformations. *Annu. Rev. Biochem.* 47:251–276.

Collier, V. L., W. A. Kronert, P. T. O'Donnell, K. A. Edwards, and S. I. Bernstein. 1990. Alternative myosin hinge regions are utilized in a tissue-specific fashion that correlates with muscle contraction speed. *Genes & Dev.* 4:885–895.

Dutcher, S. K., B. Huang, and D. J. L. Luck. 1984. Genetic dissection of the central pair microtubules of the flagella of *Chlamydomonas reinhardtii*. *J. Cell Biol.* 98:229–236.

Ebersold, W. T. 1967. *Chlamydomonas reinhardti*: Heterozygous diploid strains. *Science (Wash. D.C.).* 157:446–449.

Ferris, P. J., and U. W. Goodenough. 1994. The mating-type locus of *Chlamydomonas reinhardtii* contains highly rearranged DNA sequences. *Cell.* 76:1135–1145.

Garnier, J., D. J. Osguthorpe, and B. Robson. 1978. Analysis of the accuracy and implications of simple methods for predicting the secondary structure of globular proteins. *J. Mol. Biol.* 120:97–120.

Gibbons, I. R., B. H. Gibbons, G. Mocz, and D. J. Asai. 1991. Multiple nucleotide binding sites in the sequence of the dynein β-heavy chain. *Nature (Lond.).* 352:640–643.

Goodenough, U. W., and J. E. Heuser. 1984. Structural comparison of purified dynein proteins with in situ dynein arms. *J. Mol. Biol.* 180:1083–1118.

Goodenough, U. W., and J. E. Heuser. 1989. Structure of the soluble and in situ ciliary dyneins visualized by quick-freeze deep-etch microscopy. *In* Cell Movement. Vol. 1. F. D. Warner, P. Satir, and I. R. Gibbons, editors. Alan R. Liss Inc., New York. pp. 121–140.

Harris, E. H. 1989. The *Chlamydomonas* Sourcebook. Academic Press, San Diego, CA. 780 pp.

Holzbaur, E. L. F., A. Mikami, B. M. Paschal, and R. B. Vallee. 1994. Molecular characterization of cytoplasmic dynein. *In* Microtubules. J. S. Hyams and C. W. Lloyd, editors. Wiley-Liss, Inc., New York. pp. 251–267.

Huang, B., Z. Ramanis, and D. J. L. Luck. 1982. Suppressor mutations in *Chlamydomonas* reveal a regulatory mechanism for flagellar function. *Cell.* 28:115–124.

Johnson, D. E., and S. K. Dutcher. 1991. Molecular studies of linkage group XIX of *Chlamydomonas reinhardtii*: evidence against a basal body location. *J. Cell Biol.* 113:339–346.

Kamiya, R. 1988. Mutations at twelve independent loci result in absence of outer dynein arms in *Chlamydomonas reinhardtii*. *J. Cell Biol.* 107: 2253–2258.

Kamiya, R., E. Kurimoto, H. Sakakibara, and T. Okagaki. 1989. A genetic approach to the function of inner- and outer-arm dynein. *In* Cell Movement. Vol. 1, F. D. Warner, P. Satir, and I. R. Gibbons, editors. Alan R. Liss Inc., New York. pp. 209–218.

King, S. M., T. Otter, and G. B. Witman. 1986. Purification and characterization of *Chlamydomonas* flagellar dyneins. *Methods Enzymol.* 134:291–306.

King, S. M., and G. B. Witman. 1987. Structure of the alpha and beta heavy chains of the outer dynein arms in *Chlamydomonas reinhardtii*. *J. Biol. Chem.* 262:17596–17604.

King, S. M., and G. B. Witman. 1988. Structure of the α and β heavy chains of the outer arm dynein from *Chlamydomonas reinhardtii*. Location of epitopes and protease-sensitive sites. *J. Biol. Chem.* 263:9244–9255.

King, S. M., and G. B. Witman. 1990. Localization of an intermediate chain of outer arm dynein by immunoelectron microscopy. *J. Biol. Chem.* 265: 19807–19811.

Kurimoto, E., and R. Kamiya. 1991. Microtubule sliding in flagellar axonemes missing inner- or outer-arm dynein: velocity measurements on new types of mutants by an improved method. *Cell Motil. Cytoskel.* 19:275–281.

Laemmli, U. K. 1970. Cleavage of structural proteins during the assembly of the head of bacteriophage T4. *Nature (Lond.).* 227:680–685.

Levine, R. P., and W. T. Ebersold. 1960. The genetics and cytology of *Chlamydomonas*. *Annu. Rev. Microbiol.* 14:197–216.

Li, M. G., M. McGrail, M. Serr, and T. S. Hays. 1994. *Drosophila* cytoplasmic dynein, a microtubule motor that is asymmetrically localized in the oocyte. *J. Cell Biol.* 126:1475–1494.

Luck, D. J. L., G. Piperno, Z. Ramanis, and B. Huang. 1977. Flagellar mutants of *Chlamydomonas*: studies of radial spoke-defective strains by dikaryon and revertant analysis. *Proc. Natl. Acad. Sci. USA.* 74:3456–3460.

Luck, D. J. L., and G. Piperno. 1989. Dynein arm mutants of *Chlamydomonas*. *In* Cell Movement. Vol. 1. F. D. Warner, P. Satir, and I. R. Gibbons, editors. Alan R. Liss Inc., New York. pp. 49–60.

Lupas, A., M. Van Dyke, and J. Stock. 1991. Predicting coiled coils from protein sequences. *Sci. (Wash. DC).* 252:1162–1164.

Mastronarde, D. N., E. T. O'Toole, K. McDonald, J. R. McIntosh, and M. E. Porter. 1992. Arrangement of inner dynein arms in wild-type and mutant flagella of *Chlamydomonas*. *J. Cell Biol.* 118:1145–1162.

Mikami, A., B. M. Paschal, M. Mazumdar, and R. B. Vallee. 1993. Molecular cloning of the retrograde transport motor cytoplasmic dynein (MAP1C). *Neuron.* 10:787–796.

Mitchell, D. R., and J. L. Rosenbaum. 1985. A motile *Chlamydomonas* flagellar mutant that lacks outer dynein arms. *J. Cell Biol.* 100:1228–1234.

Mitchell, D. R. 1989. Molecular analysis of the alpha and beta dynein genes of *Chlamydomonas reinhardtii*. *Cell Motil. Cytoskel.* 14:435–445.

Mitchell, D. R., and Y. Kang. 1991. Identification of *oda6* as a *Chlamydomonas* dynein mutant by rescue with the wild-type gene. *J. Cell Biol.* 113:835–842.

Mitchell, D. R., and Y. Kang. 1993. Reversion analysis of dynein intermediate chain function. *J. Cell Sci.* 105:1069–1078.

Mitchell, D. R., and K. Brown. 1994. Sequence analysis of the *Chlamydomonas* alpha and beta dynein heavy chain genes. *J. Cell Sci.* 107:635–644.

Mocz, G., and I. R. Gibbons. 1993. ATP-insensitive interaction of the amino-terminal region of the beta heavy chain of dynein with microtubules. *Biochemistry.* 32:3456–3460.

Neville, D. M. 1971. Molecular weight determination of protein-dodecyl sulfate complexes by gel electrophoresis in a discontinuous buffer system. *J. Biol. Chem.* 246:6328–6334.

Ogawa, K. 1991. Four ATP-binding sites in the midregion of the β heavy chain of dynein. *Nature (Lond.).* 352:643–645.

Piperno, G., and D. J. L. Luck. 1979. Axonemal adenosine triphosphatases from flagella of *Chlamydomonas reinhardtii*. *J. Biol. Chem.* 254:3084–3090.

Piperno, G., K. Mead, and W. Shestak. 1992. The inner dynein arms I2 interact with a "dynein regulatory complex" in *Chlamydomonas* flagella. *J. Cell Biol.* 118:1455–1464.

Porter, M. E., J. M. Scholey, D. L. Stemple, G. P. A. Vigers, R. D. Vale, M. P. Sheetz, and J. R. McIntosh. 1987. Characterization of the microtubule movement produced by sea urchin egg kinesin. *J. Biol. Chem.* 262: 2794–2802.

Porter, M. E., and K. A. Johnson. 1989. Dynein structure and function. *Annu. Rev. Cell Biol.* 5:119–151.

Porter, M. E., J. Power, and S. K. Dutcher. 1992. Extragenic suppressors of paralyzed flagellar mutations in *Chlamydomonas reinhardtii* identify loci that alter the inner dynein arms. *J. Cell Biol.* 118:1163–1176.

Porter, M. E., and K. A. Johnson. 1983. Characterization of the ATP-sensitive binding of *Tetrahymena* 30S dynein to bovine brain microtubules. *J. Biol. Chem.* 258:6575–6581.

Ranum, L. P. W., M. D. Thompson, J. A. Schloss, P. A. Lefebvre, and C. D. Silflow. 1988. Mapping flagellar genes in *Chlamydomonas* using restriction fragment length polymorphisms. *Genetics.* 120:109–122.

Sakakibara, H., D. R. Mitchell, and R. Kamiya. 1991. A *Chlamydomonas* outer arm dynein mutant missing the alpha heavy chain. *J. Cell Biol.* 113:615–622.

Sakakibara, H., S. Takada, S. M. King, G. B. Witman, and R. Kamiya. 1993. A *Chlamydomonas* outer arm mutant with a truncated β heavy chain. *J. Cell Biol.* 122:653–661.

Sambrook, J., E. F. Fritsch, and T. Maniatis. 1989. Molecular Cloning: A Laboratory Manual. 2nd ed. Cold Spring Harbor Laboratory Press, Cold Spring Harbor, NY. pp. 9.31–9.55.

Smith, E. F., and W. S. Sale. 1992. Regulation of dynein-driven microtubule

sliding by the radial spokes in flagella. *Science (Wash. DC).* 257:1557–1559.
Smith, E. F., and W. S. Sale. 1994. Mechanisms of flagellar movement: functional interactions between dynein arms and the radial spoke-central apparatus complex. *In* Microtubules. J. Hyams and C. Lloyd, editors. Wiley-Liss, Inc., New York. pp. 381–392.
Stewart, R. J., J. P. Thaler, and L. S. B. Goldstein. 1993. Direction of microtubule movement is an intrinsic property of the motor domains of kinesin heavy chain and *Drosophila* ncd protein. *Proc. Natl. Acad. Sci. USA.* 90: 5209–5213.
Uyeda, T. Q. P., and J. A. Spudich. 1993. A functional recombinant myosin II lacking a regulatory light-chain binding site. *Science (Wash. DC).* 262: 1867–1870.
Vale, R. D., and Y. Y. Toyoshima. 1988. Rotation and translocation of microtubules in vitro induced by dyneins from *Tetrahymena* cilia. *Cell.* 52:459–469.
Vallee, R. 1993. Molecular analysis of the microtubule motor dynein. *Proc. Natl. Acad. Sci. USA.* 90:8769–8772.
Vallee, R. B., J. S. Wall, B. M. Paschal, and H. S. Sheptner. 1988. Microtubule-associated protein 1C from brain is a two headed cytosolic dynein. *Nature (Lond.).* 332:561–563.
Waxman, L., and A. Goldberg. 1982. Protease La from *Escherichia coli* hydrolyzes ATP in a linked fashion. *Proc. Natl. Acad. Sci. USA.* 79:4883–4887.
Williams, B. D., D. R. Mitchell, J. R. Rosenbaum. 1986. Molecular cloning and expression of flagellar radial spoke and dynein genes of *Chlamydomonas. J. Cell Biol.* 103:1–11.
Wilkerson, C. G., S. M. King, and G. B. Witman. 1994. Molecular analysis of the γ heavy chain of *Chlamydomonas* flagellar outer arm dynein. *J. Cell Sci.* 107:497–506.
Witman, G. B. 1986. Isolation of *Chlamydomonas* flagella and flagellar axonemes. *Methods Enzymol.* 134:280–290.
Witman, G. B., K. A. Johnson, K. K. Pfister, and J. S. Wall. 1983. Fine structure and molecular weight of the outer arm dyneins of *Chlamydomonas. J. Submicrosc. Cytol.* 15:193–197.